Pakistan Veterinary Journal

ISSN: 0253-8318 (PRINT), 2074-7764 (ONLINE)
DOI: 10.29261/pakvetj/2025.298

RESEARCH ARTICLE

Molecular Characterization and Development of Specific Monoclonal Antibodies Against Chicken CD86

Shuangjiang He[1, 2#], Shi Yin[1, 2#], Huining Zhang[1, 2], Chuang Meng[5], Jing Cao[1, 2], Hui Li[1, 2], Xiaoli Hao[1, 2*] and Shaobin Shang[1, 2, 3, 4]

[1] College of Veterinary Medicine, Yangzhou University, Yangzhou, 225009, China; [2] Institute of Comparative Medicine, Yangzhou University, Yangzhou, 225009, China; [3]Jiangsu Co-innovation Center for Prevention and Control of Important Animal Infectious Diseases and Zoonosis, Yangzhou University, Yangzhou, 225009, China; [4] International Corporation Laboratory of Agriculture and Agricultural Products Safety, Yangzhou University, Yangzhou, 225009, Jiangsu, China; [5] Jiangsu Key Laboratory of Zoonosis, Yangzhou University, Yangzhou 225009, China.
[#]These authors equally contributed.
*Corresponding author: xlhao@yzu.edu.cn

ARTICLE HISTORY (25-641)

Received: August 07, 2025
Revised: October 13, 2025
Accepted: October 19, 2025
Published online: November 25, 2025

Key words:
Chicken CD86
Flow cytometry
Monoclonal antibodies
Phylogenetic analysis

ABSTRACT

CD86, a costimulatory molecule expressed on antigen-presenting cells, critically modulates T cell activation via specific binding to CD28 or CTLA-4 on T cells. Although human and murine CD86 are well-characterized, avian CD86 remains unidentified and uncharacterized due to the lack of specific antibodies. In this study, we cloned and expressed the chicken CD86 (chCD86) gene, generated specific monoclonal antibodies (mAbs) against it, and characterized its expression pattern on chicken immune cells. Phylogenetic analysis showed that chCD86 has less than 35% amino acid homology with its mammalian counterparts. Recombinant chCD86 protein (rchCD86) was expressed in both *E. coli* and DF-1 cells, respectively, and the purified prokaryotic rchCD86 was used as an immunogen to generate three mAbs against chCD86. These mAbs can recognize natural chCD86 expressed on chicken monocytes/macrophages, as confirmed by indirect immunofluorescence assay (IFA) and Western blotting. Furthermore, flow cytometric analysis demonstrated that all mAbs detect chCD86 expression on approximately 7% of chicken KUL01$^+$ leukocytes. Overall, we generated specific mAbs against chCD86 and delineated its expression profile on chicken immune cells. These reagents provide essential immunological tools for further investigation into the roles of chCD86-expressing cells in diseases and immunity.

To Cite This Article: He S, Yin S, Zhang H, Meng C, Cao J, Li H, Hao X and Shang S, 2025. Molecular characterization and development of specific monoclonal antibodies against chicken CD86. Pak Vet J, 45(4): 1903-1911. http://dx.doi.org/10.29261/pakvetj/2025.298

INTRODUCTION

CD86 (B7-2), a member of the B7 family, serves as a critical costimulatory molecule expressed on antigen-presenting cells (APCs), including dendritic cells (DCs), macrophages, and B cells (Collins *et al.*, 2005; Cutolo *et al.*, 2022; Zhang *et al.*, 2023; Winter *et al.*, 2024). It specifically binds to CD28 or cytotoxic T lymphocyte-associated antigen 4 (CTLA-4) on T cells(Podlesnykh *et al.*, 2021; Zhao *et al.*, 2023). These receptors are shared with CD80 (B7-1), with which CD86 can form heterodimers (Tekguc *et al.*, 2021; Kennedy *et al.*, 2022). CD86 primarily delivers the second signal required for T cell activation and proliferation, a process dependent on two-signal transduction(Thiel *et al.*, 2009). The first signal arises from the interaction between the antigen-specific T cell receptor (TCR) and the peptide-MHC complex on APCs, initiating T cell activation without promoting proliferation or cytokine secretion(Bernard *et al.*, 2002). Ligation of CD86 to CD28 transmits the costimulatory signal, driving T cell proliferation and differentiation (Magee *et al.*, 2012; Hwang *et al.*, 2020). Conversely, CD86 binding to CTLA-4 delivers inhibitory signals to T cells (Collins *et al.*, 2005; Kennedy *et al.*, 2022; Oxley *et al.*, 2024).

CD86 plays critical roles in adaptive immunity, tumor immunity, autoimmune diseases, and transplant rejection(Latek *et al.*, 2009; Peng *et al.*, 2013; Gan *et al.*, 2022; Neppelenbroek *et al.*, 2024). For example, in rheumatoid arthritis, CD86-CD28 interaction promotes

pathogenic T cell activation and proliferation (Yamada *et al.*, 2002; Maehara *et al.*, 2024). In various cancers (e.g., breast, colorectal), elevated CD86 expression correlates with immune cell infiltration and anti-tumor responses (Sato *et al.*, 2022; Ikeda *et al.*, 2023; Zhang *et al.*, 2023; Ke *et al.*, 2024). Furthermore, CD86-mediated T cell activation contributes significantly to transplant rejection (Rogers *et al.*, 2000; Tadaki *et al.*, 2000). Upregulation of CD86 on porcine DCs during porcine reproductive and respiratory syndrome virus (PRRSV) infection modulates T cell activation and the antiviral immune response(Park *et al.*, 2008; Cecere *et al.*, 2012; Richmond *et al.*, 2015). These findings highlight the importance of CD86 in mammalian immunity and its potential as a therapeutic target. However, the role of CD86 in immune-related diseases of poultry has not been reported.

In human, the *CD86* gene consists of 990 nucleotides, encoding a protein of 329 amino acids (aa) with a signal peptide located at the first 23aa. The mature chain comprises 306 aa, with an extracellular domain (224aa), a transmembrane helix (21aa) and an intracellular domain (61aa), as annotated in UniProt (Protein entry: P42081). CD86 is a glycosylated protein with a molecular weight of approximately 70kDa and contains 8 potential N-glycosylation sites. While mammalian CD86 is well-characterized (Jeannin *et al.*, 1997; Axelsson *et al.*, 2020), its avian ortholog had not been identified or functionally characterized, being only genomically annotated.

In this study, we cloned the chCD86 gene and characterized its phylogenetic relationships and molecular features. Using specific anti-chCD86 monoclonal antibodies (mAbs) generated against recombinant protein, we detected native chCD86 expression on chicken monocytes/macrophages. Characterization revealed an apparent molecular mass of approximately 60kDa by Western blotting and a frequency of approximately 7% among gated KuL01$^+$ leukocytes by flow cytometry. This study reports the pioneering identification and characterization of CD86 in birds and demonstrates that the generated mAbs are suitable for flow cytometric detection of chCD86-expressing cells, providing essential tools for investigating its role in avian immunity and disease.

MATERIALS AND METHODS

Animals, cell lines and antibodies: ICR and 5-week-old BALB/c mice were obtained from Comparative Medicine Center of Yangzhou University. Four-week-old specific-pathogen-free (SPF) White Leghorn chickens were purchased from Zhejiang Lihua Agricultural Technology Co., Ltd (Ningbo, China). Mouse myeloma cell line SP2/0 and chicken fibroblast cell line DF-1 were provided by Dr. Jianqiang Ye at Yangzhou University. Anti-His Mouse Monoclonal Antibody was purchased from TransGen Biotech Co., Ltd (Beijing, China), and Mouse Anti-Chicken Monocyte/Macrophage (KUL01) (15H6) conjugated with PE was purchased from SouthernBiotech (Birmingham, AL, USA).

Isolation of peripheral blood mononuclear cells, mRNA extraction and gene cloning: Chicken peripheral blood mononuclear cells (PBMCs) were isolated with a separation kit for chicken PBMCs (TBD, Tianjin, China) as per our previous protocol(He *et al.*, 2022). In brief, the blood was diluted in phosphate buffered saline (PBS) containing 2% fetal bovine serum (FBS) (Gibco, Grand Island, NY, USA) (1:1), and then overlaid onto the blood separation solution (TBD, Tianjin, China) at a 1:1 ratio and centrifuged at 500g for 30min at room temperature (RT). The mononuclear cells at interface were collected and washed. Finally, the cells were resuspended in complete RPMI1640 medium containing 5% chicken serum, 5% FBS (Gibco, Grand Island, NY, USA), penicillin (100U/ml) and streptomycin (0.1mg/ml) (Beyotime, Shanghai, China).

The isolated PBMCs were seeded in 6-well plate with 2×10^7 cells per well in 2mL complete RPMI 1640 medium and cultured for 12h. The adherent cells were harvested for mRNA extraction and cDNA reverse transcription. Total RNA was extracted using FastPure Cell/Tissue Total RNA Isolation Kit (Vazyme, Nanjing, China) and reverse transcribed into cDNA with HiScript III RT SuperMix for qPCR (Vazyme, Nanjing, China) according to the specification. To obtain the full-length ch*CD86* gene sequence, a pair of primers based on CD86 gene (Genbank accession num: NM_001037839.1) were designed: Forward, 5'-CCGGAATTC(*EcoRI*)ATGGAGGTCTGCATATTCTTTCT-3'; Reverse, 5'-CCGCTCGAG(*XhoI*)TTAGACTGCGAGACTGACACT-3'. Finally, the amplified polymerase chain reaction (PCR) product (the full-length ch*CD86* gene) was cloned into a pMD19-T vector (TaKaRa, Shiga, Japan) and confirmed by DNA sequencing.

2.3 Sequence characteristics and phylogenetic analysis: Chicken CD86 nucleotide (Genbank accession num: NM_001037839.1) and protein (Genbank accession num: NP_001032928.1) sequence were obtained from National Center for Biotechnology Information (NCBI). The protein sequence was analyzed using the ExPASy Molecular Biology Server (http://www.expasy.ch/tools/), the extracellular region was predicted by TMHMM-2.0 (https://dtu.biolib.com/DeepTMHMM), and the potential N-glycosylation sites were obtained from NetNGlyc 1.0 Server (https://services.healthtech.dtu.dk/services/NetNGlyc-1.0/). BioEdit software (7.2.1) with CLUSTAL W algorithm was used for protein sequence analysis. Maximum likelihood phylogeny was drawn with MEGA 6 software (6.06), and bootstrap support for each node was evaluated with 1,000 replicates.

Recombinant expression of chCD86 in E. coli: Recombinant expression in *E. coli* was performed according to our previous protocol(He *et al.*, 2022). The extracellular domain sequence of ch*CD86* gene was cloned into pET-28a plasmid with a pair of primers (Forward: 5'-CGGGATCC(*BamHI*) AACGTACATCACGTGAAGTCA-3' and Reverse: 5'-CCGCTCGAG(*XhoI*)TCAATTTACCTTCACCGGTTCCAT-3') and transformed into *E. coli* BL21 (DE3) strain for recombinant expression by inducing with 0.1mM Isopropyl β-D-Thiogalactoside (IPTG) (Solarbio, Beijing, China) at 37°C. The bacteria were harvested after 4h induction, subjected to 12% sodium dodecyl sulfate polyacrylamide gel electrophoresis (SDS-PAGE), and analyzed by Coomassie

Blue (Beyotime, Shanghai, China). In order to obtain adequate recombinant chCD86 (rchCD86), 200mL bacteria culture was induced at the above condition. The bacteria pellets were collected, sonicated, and dissolved with 8M urea. The rchCD86 with his tag was purified with the Ni Sepharose Column (General Electric, Boston, MA, USA) under denature condition according to the specification. The purified rchCD86 was refolded by dialysis with gradient urea buffer (4, 3, 2, 1, 0M) at 4°C, and finally quantified by BCA Protein Assay Kit (Beyotime, Shanghai, China).

Transfection and indirect immunofluorescence assay: The chCD86 CDS from T-vector was cloned into pCAGGS plasmid by PCR with following primers: Forward, 5'-CCGGAATTC(*EcoRI*)ATGGAGGTCTGCATATTCTTTCT-3'; Reverse, 5'-CCGCTCGAG(*XhoI*)TTAGACTGCGAGACTGACACT-3'. The ultrapure plasmid pCAGGS and pCAGGS-chCD86-his was used to transfection with Lipofectamine™ 2000 Reagent (Invitrogen, Carlsbad, CA, USA) according to the specification. In brief, the DF-1 cells (2×10^4/well) were seeded in a 96-well plate, and then were transfected with plasmid pCAGGS or pCAGGS-chCD86-his along with Lipofectamine® Reagent (0.25μL/well). After cultured for 48 h, the plate with transfected cells was subjected to indirect immunofluorescence assay (IFA). The transfected cells were fixed with ice cold acetone-ethanol mixture (3:2) for 5min, and blocked with 5% skimmed milk (Beyotime, Shanghai, China) in phosphate buffered saline (PBS) for 2h at RT. Afterwards, the cells were washed and incubated with Anti-his mouse monoclonal antibody (mAb) (TransGen Biotech, Beijing, China) (1:500) for 2h at 37°C. After three washed with PBS, the cells were incubated with Goat Anti-Mouse IgG H&L (Alexa Fluor® 488) (abcam, Cambridge, UK) (1:1000) for 1h at RT. Finally, the cells were observed under the inverted fluorescence microscope (NIKON, Shanghai, China).

The generation of monoclonal antibodies against chCD86: The procedure of anti-chCD86 mAbs generation and Enzyme-Linked Immunosorbent Assay (ELISA) were performed in accordance with our previous protocol(He *et al.*, 2022). In brief, prokaryotic rchCD86 (50μg) was used as an immunogen to immunize 5-week-old BALB/c mice three times at two-week intervals, along with Freund's adjuvant (Sigma-Aldrich, Poole, UK) via intraperitoneal injection. After booster immunization, hybridomas were obtained by the fusion of splenocytes from immunized mice with SP2/0 cells in the presence of PEG1500 (Roche, Mannheim, Germany) at 37°C. These hybridomas were then cultured in DMEM complete culture medium (Gibco, Grand Island, NY, USA) containing hypoxanthine, aminopterin and thymidine (HAT) (Thermo Fisher Scientific, Waltham, MA, USA) for 10 days. Positive hybridomas were screened using prokaryotic rchCD86 by ELISA, and then cloned twice by limiting dilution methods. The stable hybridomas secreting anti-chCD86 mAbs were generated, and further characterized by IFA for its reactivity with eukaryotic rchCD86 expressed in DF-1 cells and Western blot for its reactivity to prokaryotic rchCD86. The IgG subclass and light chain class of all anti-chCD86 mAbs were determined with the Mouse Immunoglobulin Isotyping ELISA Kit (BD Biosciences, Franklin Lakes, NJ, USA).

The reactivity of mAbs with natural chCD86 identified by indirect immunofluorescence assay and Western blot: The separated PBMCs (2×10^6/well) were seeded in 96-well plate, and cultured for 12h in cell incubator at 37°C, 5% CO_2. The suspended cells were removed, and the adherent cells were fixed and blocked. Afterwards, the cells were washed and incubated with anti-chCD86 mAbs or negative serum (Control) for 2h at 37°C. After washed with PBS, the cells were incubated with Alexa Fluor® 488-conjugated anti-mouse IgG (abcam, Cambridge, UK) and DAPI Staining Solution (Beyotime, Shanghai, China). Finally, the immunofluorescence was observed under the inverted fluorescence microscope.

The separated PBMCs (20×10^6/well) were seeded in 6-well plate, and cultured for 12h. The obtained adherent cells were lysed in RIPA lysis buffer (NCM Biotech, Suzhou, China), and the total protein was harvested and quantified. The protein was mixed with 5×SDS-PAGE Loading Buffer (reducing) and boiled in boiling water for 5min. 30μg total protein or 3μL pre-stained protein ladder (Vazyme, Nanjing, China) was loaded to each lane and subjected to 12% SDS-PAGE at 100V. Afterwards, the protein in gel was transferred to polyvinylidene fluoride (PVDF) membrane (Millipore, MA, USA) at 200mA for 90min. The PVDF membranes were blocked with 5% skim milk and then incubated with various anti-chCD86 mAbs overnight at 4°C. After washed with Tris Buffered Saline (TBS) containing 0.5% Tween 20 (TBS-T), all the membranes were incubated with HRP-conjugated anti-mouse IgG antibody (TransGen Biotech, Beijing, China) for 1h at 37°C. Finally, the targeted band was developed with enhanced chemiluminescence substrate (NCM Biotech, Suzhou, China) and visualized with an electrochemiluminescence detection system (Tanon, Shanghai, China).

The reactivity of mAbs with natural chCD86 identified by Flow cytometry: The adherent cells from PBMCs were digested with 0.25% Trypsin-EDTA for 5min, and collected. The cells were washed twice with PBS, and plated in the 96-well V-bottom plate with 100μL 0.5% BSA. The cells were centrifuged and incubated with various anti-chCD86 mAbs or its isotype mAbs for 30 min at RT, respectively. Afterwards, Alexa Fluor® 647 Goat anti-mouse IgG (minimal x-reactivity) Antibody (BioLegend, San Diego, CA, USA) were then stained for 20min at RT. The cells were centrifuged and washed for 3 times, and incubated Mouse Anti-Chicken Monocyte/Macrophage (KUL01) mAb (15H6) conjugated with PE for 30min at RT. The cells were washed and resuspended in PBS for Flow cytometry with a FACS LSRFortessa (BD Biosciences, Franklin Lakes, NJ, USA). The data were analyzed by FlowJo software (Tree Star Inc., Ashland, OR, USA).

RESULTS

Sequence characteristics and phylogenetic analysis of chicken CD86: Based on the gene sequence from NCBI, an 852bp chCD86 cDNA was cloned, which encodes a cleavable signal peptide (aa 1-19) and a mature chain of 264aa with a predicted molecular mass of 29.6kDa.

Furthermore, the transmembrane helix of chCD86 is predicted to be between 247 - 267aa, the part before which is assumed to be the extracellular domain. In addition, there are eight Asparagine (Asn) residues at positions of 29, 80, 127, 131, 152, 175, 196, 271 of the chain, all of which are the potential N-glycosylation sites in the mature chCD86.

Compared with representative CD86 sequences from turkey and mammals, chCD86 displays 91.9% aa similarity to turkey but only has 29-35% homology to mammalian counterparts, with no conserved regions (Fig. 1A and Table 1). In addition, chicken or turkey CD86 is shorter in length at N-terminal or C-terminal of the protein compared to mammalian CD86s (Fig. 1A). Moreover, phylogenetic analysis indicated that chicken and turkey CD86s formed a distinct cluster far away from mammalian CD86s, reflecting the evolutionary relationship of CD86 between birds and mammals (Fig. 1B).

Table 1: Comparison of amino acid homology of chicken CD86 with other animals.

Species	Homology (%)
Turkey	91.9
Human	34.1
Mouse	29.6
Rat	30.2
Pig	33.3

Table 2: The anti-chCD86 monoclonal antibodies were characterized by indirect immunofluorescence assay (IFA), Western blot and flow cytometry (FCM). IFA analyzed the reactivity of mAbs with eukaryotic or natural chCD86, and Western blot identified the specificity of mAbs to prokaryotic or natural chCD86. FCM identified the reactivity of mAbs with natural chCD86 expressed on macrophages. -, no reaction; +, reaction.

mAb	Isotype	Ascites titre	IFA rchCD86	IFA chCD86	Western blot his-chCD86	Western blot chCD86	FCM chCD86
1C2	IgG2b, κ	1:409600	+ + +	+ + +	++	++	++
1D3	IgG1, κ	1:409600	+	++	++	++	++
3C3	IgG1, κ	1:409600	+ +	+	++	++	+++

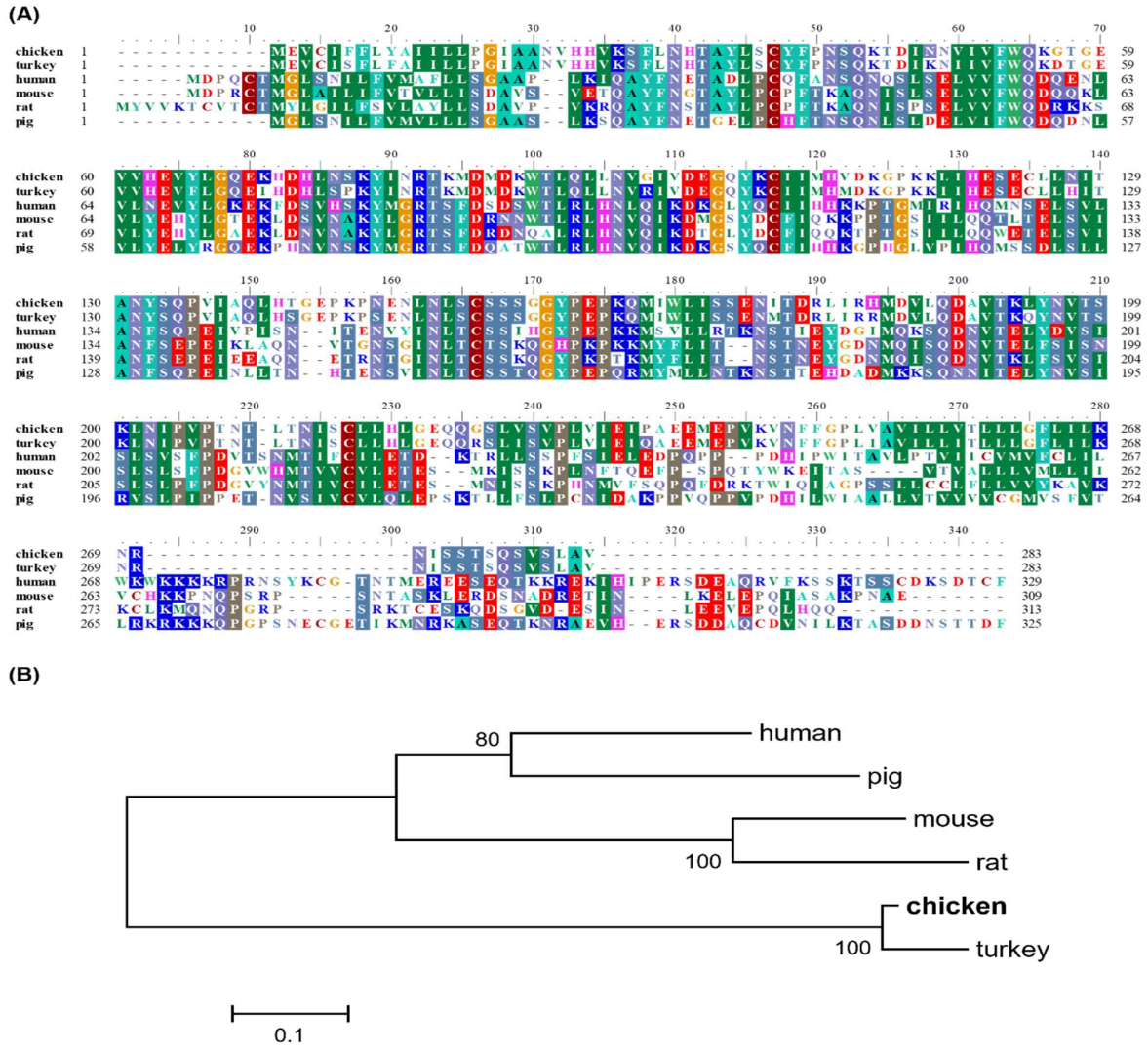

Fig. 1: Sequence alignment and phylogenetic analysis of chicken CD86 with the counterparts of other vertebrates. The GenBank accession numbers of vertebrate CD86 proteins are as follow: chicken (*Gallus*; NP_001032928.1), turkey (*Meleagris gallopavo*; XP_031411676.1), human (*Homo sapiens*; ABK41931.1), mouse (*Mus musculus*; NP_062261.3), rat (*Rattus norvegicus*; NP_064466.1), pig (*Sus scrofa*; AAB61307.1). (A) The sequence alignment was performed with BioEdit software with CLUSTAL W algorithm. (B) The phylogenetic analysis of chCD86 with other animals was performed with MEGA 6 software. The maximum likelihood tree was constructed and Bootstrap support values are shown for each node. The scale bar indicates the number of amino acid substitutions per site.

Prokaryotic and eukaryotic expression of recombinant chCD86: For prokaryotic expression, the extracellular region of chCD86 gene was amplified and cloned into the pET-28a vector (pET-28a-chCD86) (Fig. S1A, B). The recombinant plasmid was then transformed into *E. coli*. After induction with IPTG, SDS-PAGE analysis showed that rchCD86, tagged with a His-tag and with a molecular weight of approximately 30kDa, was expressed as inclusion bodies. (Fig. 2A). The fused rchCD86 protein was purified using Ni-NTA resin and refolded to a soluble protein (Fig. 2B).

For eukaryotic expression, the full-length chCD86 gene was amplified and inserted into pCAGGS vector (pCAGGS-chCD86-his) (Fig. S1A, C). The recombinant plasmid was purified and transfected into DF-1 cells. The IFA result indicated that rchCD86 was successfully expressed in DF-1 cells (Fig. 3).

The generation and characterization of anti-chCD86 mAbs: Using prokaryotic rchCD86 as an immunogen, three mouse hybridoma cells that stably secrete anti-chCD86 mAbs were generated, namely 1C2, 1D3 and 3C3. Immunoglobulin subclass and isotyping showed that mAb 1D3 and 3C3 are IgG1 and κ chain, and mAb 1C2 is IgG2b and κ chain, respectively (Table 2). Western blot analysis indicated that these mAbs specifically reacted with prokaryotic rchCD86 (Fig. S2 and Table 2). Furthermore, IFA showed that all three mAbs could specifically recognize eukaryotic rchCD86 in transfected DF-1 cells (Fig. 4 and Table 2). These results suggest that three mAbs are chCD86-specific and may have the potential to recognize natural chCD86.

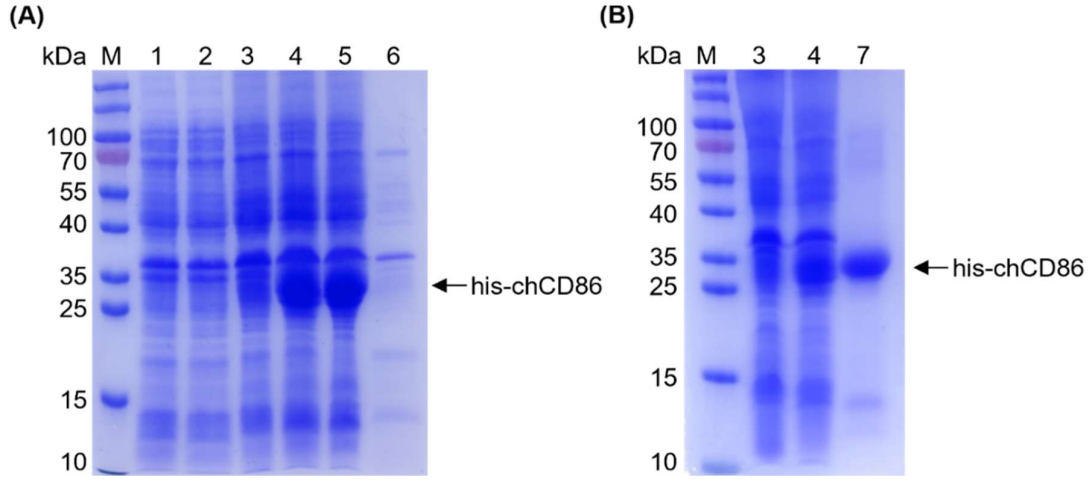

Fig. 2 The expression and purification of recombinant chCD86 in *E. coli*. The pET-28a-chCD86 plasmid was transformed into *E. coli* BL21 strain and induced by IPTG for 4h. The cells were ultrasonically crushed for expression analysis and purification of rchCD86. (A) The lysate supernatant or precipitate of uninduced or IPTG-induced *E. coli* was analyzed by SDS-PAGE, respectively. M, pre-stained protein ladder; lane 1 and 2, the lysates of uninduced and induced *E. coli* transformed with the pET-28a vector; lane 3 and 4, the lysates of uninduced and induced *E. coli* transformed with the pET-28a-chCD86 vector; lane 5 and 6, lysate precipitate and supernatant of IPTG-induced *E. coli* transformed with the pET-28a-chCD86 vector. (B) rchCD86 was purified from the inclusion body of IPTG-induced *E. coli* and confirmed by SDS-PAGE. lane 7, purified rchCD86.

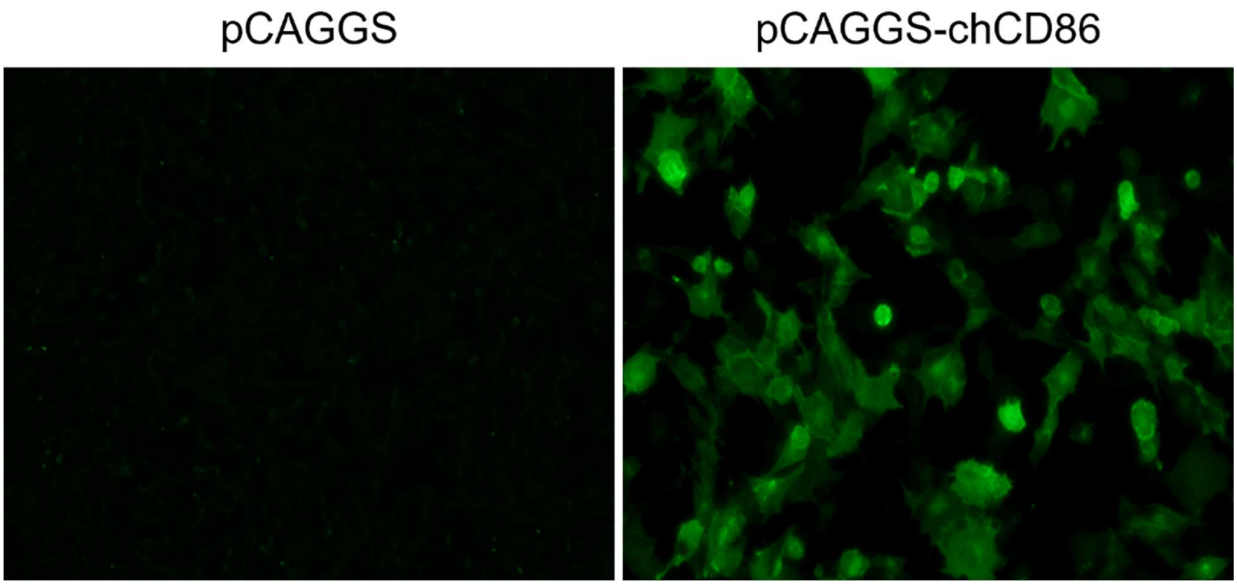

Fig. 3: Eukaryotic rchCD86 was expressed in DF-1 cells and identified by indirect immunofluorescence assay (IFA). The pCAGGS-chCD86-his plasmid was transfected into DF-1 cells, and expression analysis of rchCD86 was performed by IFA. The eukaryotic rchCD86 was recognized by anti-his mAb. The images with magnification 200× are presented.

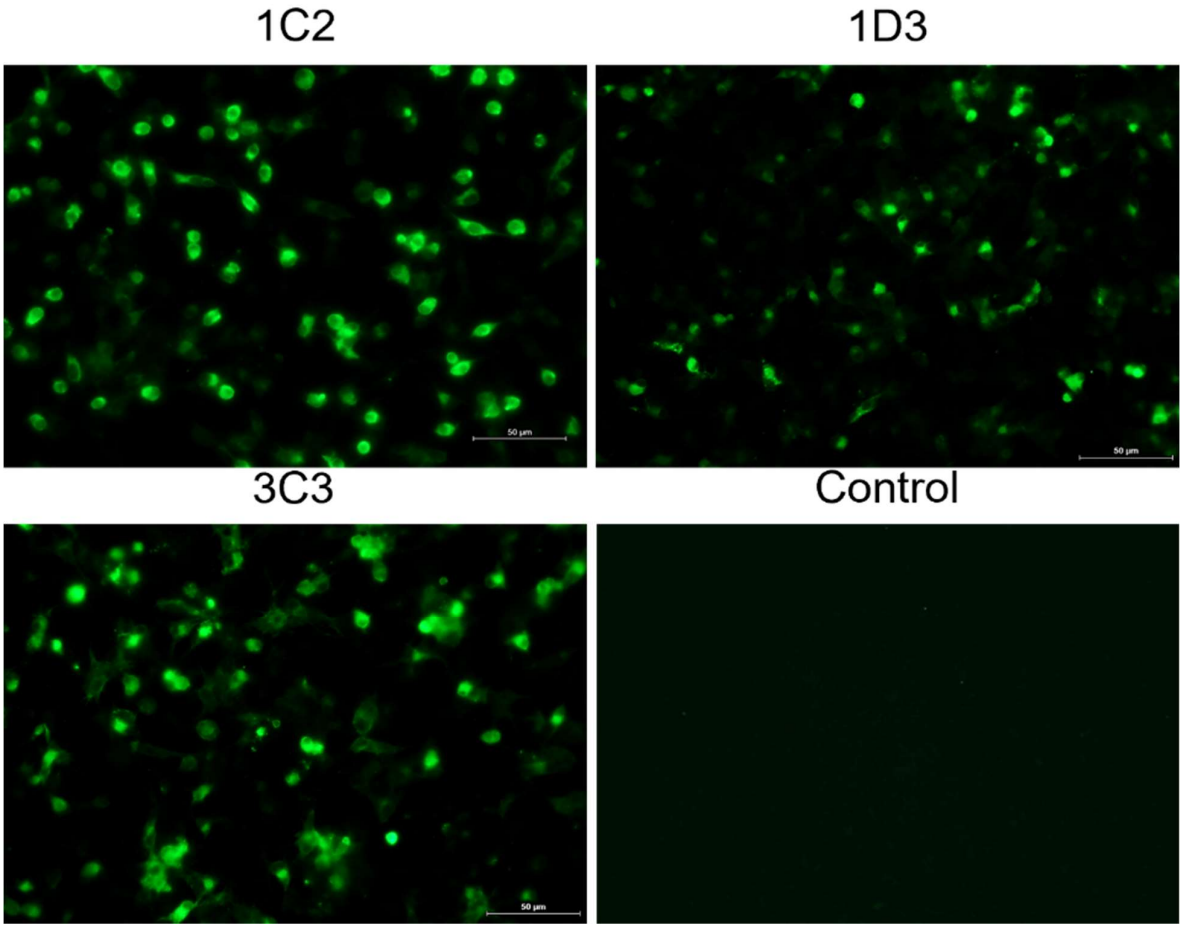

Fig. 4: The reactivity of mAbs with eukaryotic rchCD86 expressed in DF-1 cells was identified by indirect immunofluorescence assay (IFA). The purified pCAGGS-chCD86 plasmid was first transfected into DF-1 cells. After 48 h, the cells were fixed and incubated with three anit-chCD86 mAbs (1C2, 1D3 and 3C3) and mouse negative serum (Control), respectively. The reactivity was finally examined by IFA. The images with magnification 200× are presented.

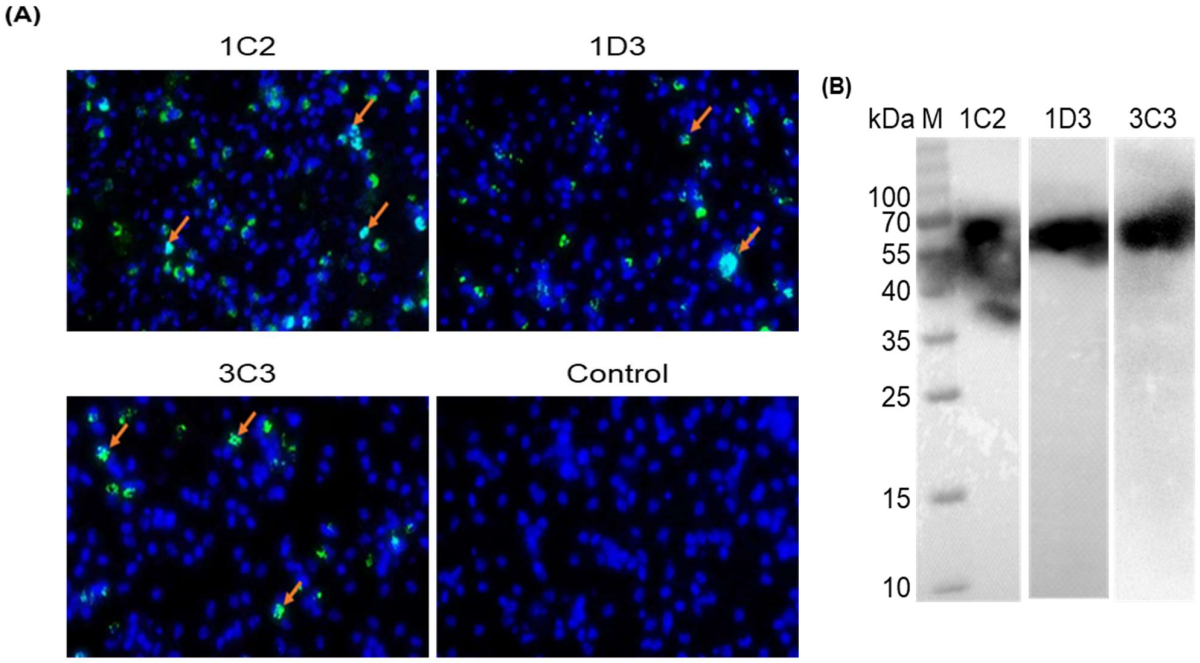

Fig. 5: The reactivity of mAbs with natural chCD86 expressed on monocytes/macrophages. (A) The cells were isolated and fixed on the bottom of 96-well plate. The reactivity of three anit-chCD86 mAbs (1C2, 1D3 and 3C3) and mouse negative serum (Control) with natural chCD86 expressed on adherent monocytes/macrophages was examined by IFA. The images with magnification 400× are presented. (B) The total protein obtained from adherent monocytes/macrophages was subjected to SDS-PAGE and Western blot. The band was recognized by anti-chCD86 mAbs.

The characterization of natural chCD86: It has been reported that CD86 is expressed on APCs such as macrophages and DCs(Chen *et al.*, 2022). To identify natural chCD86 on macrophages, the adherent monocytes/macrophages were incubated with three anti-chCD86 mAbs, respectively and subjected to indirect immunofluorescence assay (IFA). The results showed that all three mAbs have specific reactivity (Fig. 5A), indicating the presence of natural chCD86 on the chicken monocytes/macrophages. Moreover, the molecular weight of chCD86 was confirmed by Western blotting. The results indicated that anti-chCD86 mAbs specifically recognized a dominant band of 60kDa (Fig. 5B), implying that the natural chCD86 was potentially glycosylated due to its N-glycosylation sites. To confirm the frequency of $CD86^+$ cells in the adherent chicken monocytes/macrophages, further immunostaining and flow cytometry were performed. The results showed that the frequency of $CD86^+$ cells was only about 7% among leukocytes (Fig. 6), primarily within the monocyte/macrophage population. This suggests that these mAbs can be applied in flow cytometry.

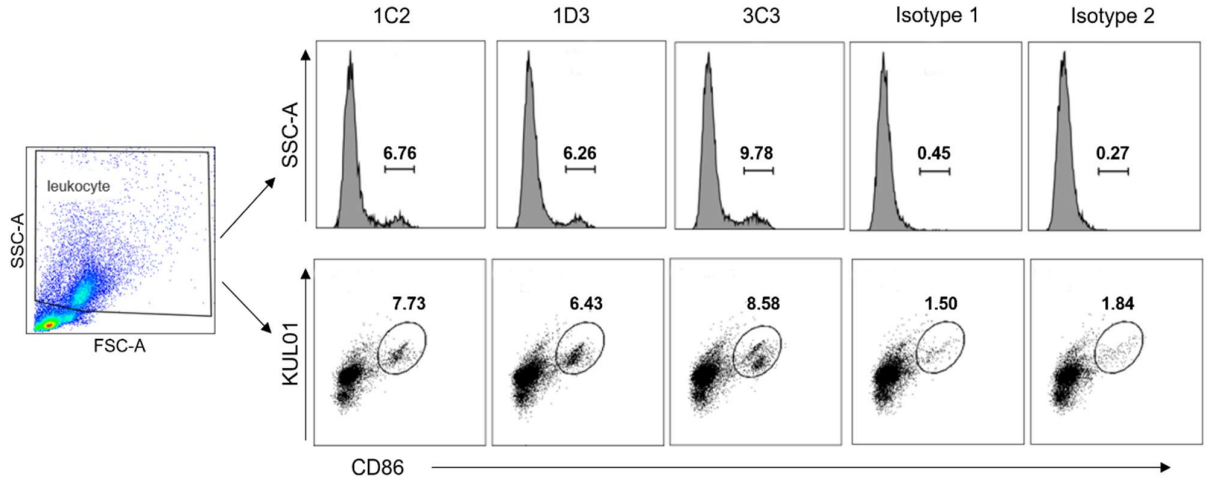

Fig. 6: Flow cytometry analysis of chCD86 expressed on the chicken monocytes/macrophages using anti-chCD86 mAbs. The adherent monocytes/macrophages from PBMCs were collected and stained with anti-chCD86 mAbs or its isotype mAbs and Mouse Anti-Chicken Monocyte/Macrophage (KUL01) IgG conjugated with PE, and subjected to flow cytometry. The percentages of chCD86- expressed cells was analyzed by FlowJo software.

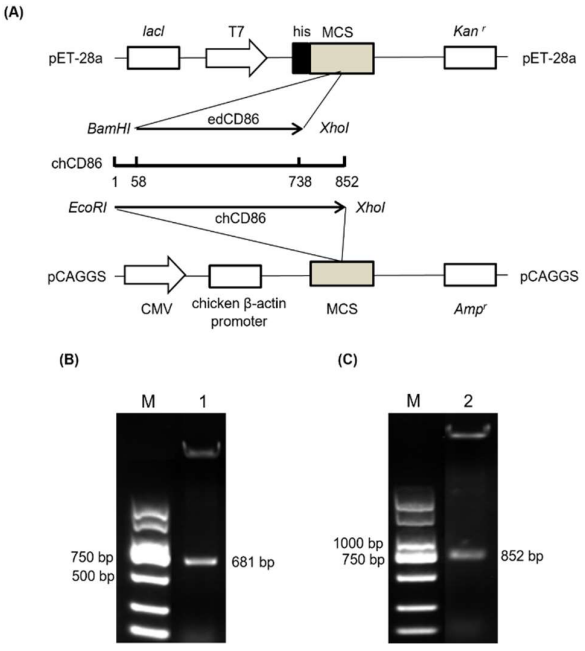

Fig. S1: Cloning and construction of recombinant plasmids pET28a-chCD86 and pCAGGS-chCD86. The extracellular (681nt) and full-length chicken *CD86* (852nt) gene were cloned into pET28a and pCAGGS vector (A), respectively. Then the constructs were confirmed by restriction enzymatic digestion (B) and (C). M, DNA ladder; lane 1, double digestion product of pET28a-chCD86; lane 2, double digestion product of pCAGGS-chCD86.

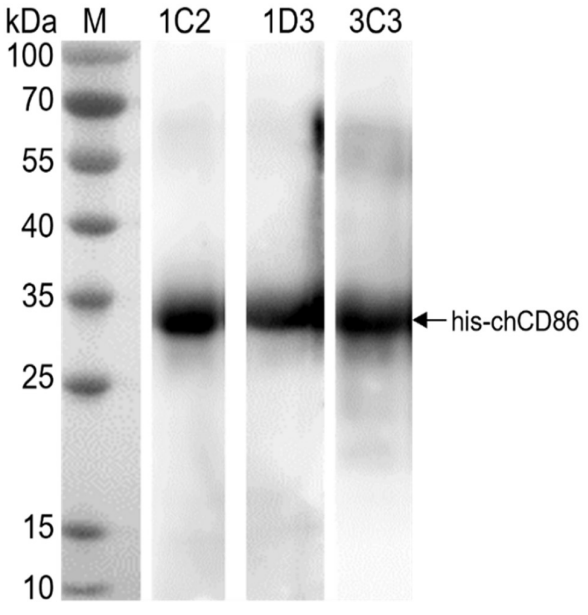

Fig. S2: The reactivity of mAbs with prokaryotic rchCD86 expressed in *E. coli* was identified by Western blot. M, pre-stained protein ladder. 1C2, 1D3 and 3C3 were chCD86 mAbs.

DISCUSSION

CD86, a B7 family costimulatory molecule, primarily delivers the second signal for T cell activation or suppression (Pereira *et al.*, 2009; Halliday *et al.*, 2020; Bandola-Simon and Roche, 2023). As a surface molecule of APCs, CD86 modulates diverse T cell functions (Thomas *et al.*, 2007; Halliday *et al.*, 2020), participating in infectious diseases, autoimmune disorders, cancer, and organ transplantation(Reiser and Stadecker, 1996; Vincenti, 2008; Dong *et al.*, 2016; Dyck and Mills, 2017; Cobankent Aytekin *et al.*, 2024; Ong *et al.*, 2024). Although mammalian CD86s have been widely investigated, avian CD86 has not yet been characterized due to the lack of immunological tools. Here, we employed gene cloning, phylogenetic analysis, recombinant expression, and anti-chCD86 monoclonal antibody (mAb) generation to identify chicken CD86. We detected natural chCD86 (~60kDa) on chicken monocytes/macrophages and demonstrated the utility of the generated mAbs for flow cytometry.

Consistent with other chicken immunomodulators (e.g., CD80, IL-9) (He *et al.*, 2022; He *et al.*, 2023), chCD86 exhibits high amino acid similarity to avian species but low homology to mammalian counterparts (Fig. 1A and Table 1). Phylogenetic analysis further confirmed that chCD86 forms a distinct evolutionary branch separate from mammalian CD86s (Fig. 1B), reflecting broader genetic divergence between birds and mammals. To prepare anti-chCD86 mAbs, we expressed the prokaryotic and eukaryotic rchCD86. Indeed, prokaryotic rchCD86 consistently formed inclusion bodies regardless of induction conditions (Fig. 2). In contrast, eukaryotic rchCD86 was highly expressed in chicken-derived DF-1 cells (Fig. 3) but minimally detectable in mammalian cell lines (e.g., COS-7, CHO, 293T; data not shown), suggesting preferential expression of chicken surface molecules in avian cell lines.

Three specific anti-chCD86 mAbs were generated. Given the low sequence homology of chCD86 with both mammalian CD86 and other chicken proteins (e.g., CD80), these mAbs are predicted to be highly specific for chCD86 with minimal cross-reactivity. Since CD86 is primarily expressed on APCs, we focused on analyzing its expression on macrophages. The generated mAbs specifically recognized not only eukaryotically expressed rchCD86 in DF-1 cells (Fig. 4), but also the native chCD86 on adherent PBMC-derived monocytes/macrophages, as confirmed by IFA (Fig. 5A). Flow cytometric analysis revealed chCD86 expression on approximately 7% of gated leukocytes, predominantly localized to $KuL01^+$ monocytes/macrophages (Fig. 6). Notably, chCD86 expression was also detected on activated B cells and dendritic cells, suggesting a broader expression profile warranting further investigation. These results confirm the suitability of the generated mAbs for flow cytometric detection of chCD86-expressing cells.

Although the co-stimulatory function of CD86 has been well established in mammals (e.g., mice and humans), its specific *in vivo* role in the avian immune system—particularly in chicken disease models—remains incompletely understood. Previous studies have demonstrated that CD86 signaling plays a dual role in immune regulation: on one hand, the co-stimulatory signal generated through its interaction with CD28 is essential for initiating effective anti-tumor and anti-infective immune responses(Barna *et al.*, 2025); On the other hand, excessive or uncontrolled CD86 co-stimulation may result in autoimmune disorders or immunopathological damage(Darvish *et al.*, 2024). Therefore, it is of great significance to investigate how CD86 regulates T-cell responses in major avian viral diseases, such as Marek's disease and avian leukosis. The development of specific agonistic or antagonistic monoclonal antibodies against chicken CD86 would provide valuable tools for elucidating the precise *in vivo* functions of chCD86 and for advancing our understanding of avian immunology.

In human, CD86 is a glycosylated protein with the molecular weight of 70kDa (329aa) and a transmembrane domain (aa 248-268), and its extracellular region contains 224aa (aa 24-247) based on UniProt Protein Data Bank. Similarly, chCD86 gene consists of a signal peptide (aa 1-19) and a mature chain of 264aa, including a transmembrane domain (aa 247-267), and an extracellular region (aa 20-246). However, in the present study, we found that chCD86 displayed a different size. Although the signal peptide-truncated rchCD86 produced in *E. coli* has a molecular weight about 30kDa (Fig. 2 and Fig. S2), the size of natural chCD86 is 60kDa (Fig. 5B), larger than the predicted molecular weight of 29.6kDa. The prepared prokaryotic recombinant protein or native protein samples were treated with reducing SDS-PAGE Loading Buffer (containing DTT) before Western blotting, which eliminated potential disulfide bonds. Additionally, glycosylation modifications are primarily found in eukaryotic cells rather than prokaryotic cells(Gomez-Gaviria *et al.*, 2021). ChCD86 possesses 8 potential N-glycosylation sites. Therefore, the observed size difference strongly indicates that native chCD86 is a highly glycosylated protein.

Conclusions: In summary, we generated and characterized three specific mAbs against chCD86, enabling its detection by IFA, Western blotting, and flow cytometry. We identified chCD86 as a likely heavily glycosylated protein with an apparent molecular mass of 60kDa. This study provides the essential immunological tools and foundational characterization for investigating the roles of chCD86 in avian immunity and disease (e.g., Marek's disease) pathogenesis.

Acknowledgments (Funding): This study was financially supported by the National Key Research and Development Program of China (2022YFD1800303), the Jiangsu Excellent Postdoctoral Program (2024ZB646), the Open Project Program of Jiangsu Key Laboratory of Zoonosis (R2401), and a project funded by the Priority Academic Program Development of Jiangsu Higher Education Institutions (PAPD) and JSSCTD202224.

Conflicts of Interest: All authors participating in this study declare that they have no potential conflicts of interest.

Ethics statement: All animal experiments were approved by Jiangsu Province Administrative Committee for

Laboratory Animals (Permission number: SYXK-SU-2021-0027), and carried out in accordance with the guidelines of Jiangsu Province Laboratory Animal Welfare and ethics of Jiangsu Province Administrative Committee of Laboratory Animals.

Authors contribution: Shuangjiang He: Data curation, Writing–original draft. Shi Yin: Data curation, Methodology. Huining Zhang: Data curation, Formal analysis. Chuang Meng: Resources. Jing Cao: Formal analysis, Validation. Hui Li: Formal analysis, Visualization. Shaobin Shang: Data curation, Writing–original draft. Xiaoli Hao: Writing–review & editing.

REFERENCES

Axelsson S, Magnuson A, Lange A, *et al*., 2020. A combination of the activation marker cd86 and the immune checkpoint marker b and t lymphocyte attenuator (btla) indicates a putative permissive activation state of b cell subtypes in healthy blood donors independent of age and sex. BMC Immunology 21(1):14.

Bandola-Simon J and Roche PA, 2023. Regulation of mhc class ii and cd86 expression by march-i in immunity and disease. Curr Opin Immunol 82: 102325.

Barna G, Szaloki G, Mark A, *et al*., 2025. Cd86, the double agent: Significance of cd86 expression in b-cell malignancies. Int J Cancer 157(9): 1772-1780.

Bernard A, Lamy and Alberti I, 2002. The two-signal model of t-cell activation after 30 years. Transplantation 73(1 Suppl): S31-35.

Cecere TE, Meng XJ, Pelzer K, *et al*., 2012. Co-infection of porcine dendritic cells with porcine circovirus type 2a (pcv2a) and genotype ii porcine reproductive and respiratory syndrome virus (prrsv) induces cd4(+)cd25(+)foxp3(+) t cells in vitro. Vet Microbiol 160(1-2): 233-239.

Chen R, Yang D, Shen L, *et al*., 2022. Overexpression of cd86 enhances the ability of thp-1 macrophages to defend against talaromyces marneffei. Immunity, Inflammation and Disease 10(12):e740.

Cobankent Aytekin E, Unal B, Bassorgun CI, *et al*., 2024. Clinicopathologic evaluation of cd80, cd86, and pd-l1 expressions with immunohistochemical methods in malignant melanoma patients. Turk Patoloji Derg 40(1): 16-26.

Collins M, Ling V and Carreno BM, 2005. The b7 family of immune-regulatory ligands. Genome Biol 6(6): 223.

Cutolo M, Campitiello R, Gotelli E, *et al*., 2022. The role of m1/m2 macrophage polarization in rheumatoid arthritis synovitis. Front Immunol 13: 867260.

Darvish Z, Kheder RK, Faraj TA, *et al*., 2024. A better understanding of the role of the ctla-cd80/86 axis in the treatment of autoimmune diseases. Cell Biochem Funct 42(1): e3895.

Dong P, Ma L, Liu L, *et al*., 2016. $Cd86^{+}/cd206^{+}$, diametrically polarized tumor-associated macrophages, predict hepatocellular carcinoma patient prognosis. Int J Mol Sci 17(3): 320.

Dyck L and Mills KHG, 2017. Immune checkpoints and their inhibition in cancer and infectious diseases. Eur J Immunol 47(5): 765-779.

Gan X, Gu J, Ju Z, *et al*., 2022. Diverse roles of immune cells in transplant rejection and immune tolerance. Engineering 10: 44-56.

Gomez-Gaviria M, Vargas-Macias AP, Garcia-Carnero LC, *et al*., 2021. Role of protein glycosylation in interactions of medically relevant fungi with the host. J Fungi (Basel) 7(10):875.

Halliday N, Williams C, Kennedy A, *et al*., 2020. Cd86 is a selective cd28 ligand supporting foxp3+ regulatory t cell homeostasis in the presence of high levels of ctla-4. Front Immunol 11: 600000.

He S, Chen L, Hao X, *et al*., 2022. First characterization of chicken interleukin-9. Front Immunol 13: 889991.

He S, Zhang H, Yin S, *et al*., 2023. Characterization of chicken interleukin-9 receptor alpha chain. Poult Sci 102(10): 102965.

Hwang J-R, Byeon Y, Kim D, *et al*., 2020. Recent insights of t cell receptor-mediated signaling pathways for t cell activation and development. Experimental & Molecular Medicine 52(5): 750-761.

Ikeda H, Nagasaki J, Shimizu D, *et al*., 2023. Immunologic significance of cd80/cd86 or major histocompatibility complex-ii expression in thymic epithelial tumors. JTO Clin Res Rep 4(10): 100573.

Jeannin P, Delneste Y, Lecoanet-Henchoz S, *et al*., 1997. Cd86 (b7-2) on human b cells. Journal of Biological Chemistry 272(25): 15613-15619.

Ke J, Chen G, You Y, *et al*., 2024. Cd11b/cd86 involved in the microenvironment of colorectal cancer by promoting wnt signaling activation. Cancer Med 13(18): e70245.

Kennedy A, Waters E, Rowshanravan B, *et al*., 2022. Differences in cd80 and cd86 transendocytosis reveal cd86 as a key target for ctla-4 immune regulation. Nature Immunology 23(9): 1365-1378.

Kennedy A, Waters E, Rowshanravan B, *et al*., 2022. Differences in cd80 and cd86 transendocytosis reveal cd86 as a key target for ctla-4 immune regulation. Nat Immunol 23(9): 1365-1378.

Latek R, Fleener C, Lamian V, *et al*., 2009. Assessment of belatacept-mediated costimulation blockade through evaluation of cd80/86-receptor saturation. Transplantation 87(6): 926-933.

Maehara Y, Takeda K, Tsuji-Yogo K, *et al*., 2024. Blockade of cd80/cd86-cd28 co-stimulation augments the inhibitory function of peptide antigen-specific regulatory t cells. Biomed Res 45(3): 115-123.

Magee CN, Boenisch O and Najafian N, 2012. The role of costimulatory molecules in directing the functional differentiation of alloreactive t helper cells. American Journal of Transplantation 12(10): 2588-2600.

Neppelenbroek S, Blomberg NJ, Kampstra ASB, *et al*., 2024. Autoreactive b cells remain active despite clinical disease control in rheumatoid arthritis. J Autoimmun 149: 103320.

Ong CEB, Lyons AB, Woods GM, *et al*., 2024. Generation of devil facial tumour cells co-expressing mhc with cd80, cd86 or 41bbl to enhance tumour immunogenicity. Parasite Immunol 46(8-9): e13062.

Oxley EP, Kershaw NJ, Louis C, *et al*., 2024. Context-restricted pd-(l)1 checkpoint agonism by ctla4-ig therapies inhibits t cell activity. Cell Rep 43(10): 114834.

Park JY, Kim HS and Seo SH, 2008. Characterization of interaction between porcine reproductive and respiratory syndrome virus and porcine dendritic cells. J Microbiol Biotechnol 18(10): 1709-1716.

Peng Y, Luo G, Zhou J, *et al*., 2013. Cd86 is an activation receptor for nk cell cytotoxicity against tumor cells. PLoS One 8(12): e83913.

Pereira C, Tavares B, Loureiro G, *et al*., 2009. Dynamics of cd86 expression on allergic inflammation--new insights. Recent Pat Inflamm Allergy Drug Discov 3(2): 128-131.

Podlesnykh SV, Abramova KE, Gordeeva A, *et al*., 2021. Peptide blocking ctla-4 and b7-1 interaction. Molecules 26(2):253.

Reiser H and Stadecker MJ, 1996. Costimulatory b7 molecules in the pathogenesis of infectious and autoimmune diseases. N Engl J Med 335(18): 1369-1377.

Richmond O, Cecere TE, Erdogan E, *et al*., 2015. The pd-l1/cd86 ratio is increased in dendritic cells co-infected with porcine circovirus type 2 and porcine reproductive and respiratory syndrome virus, and the pd-l1/pd-1 axis is associated with anergy, apoptosis, and the induction of regulatory t-cells in porcine lymphocytes. Vet Microbiol 180(3-4): 223-229.

Rogers NJ, Mirenda V, Jackson I, *et al*., 2000. Costimulatory blockade by the induction of an endogenous xenospecific antibody response. Nat Immunol 1(2): 163-168.

Sato T, Takagi K, Higuchi M, *et al*., 2022. Immunolocalization of cd80 and cd86 in non-small cell lung carcinoma: Cd80 as a potent prognostic factor. Acta Histochem Cytochem 55(1): 25-35.

Tadaki DK, Craighead N, Saini A, *et al*., 2000. Costimulatory molecules are active in the human xenoreactive t-cell response but not in natural killer-mediated cytotoxicity. Transplantation 70(1): 162-167.

Tekguc M, Wing JB, Osaki M, *et al*., 2021. Treg-expressed ctla-4 depletes cd80/cd86 by trogocytosis, releasing free pd-l1 on antigen-presenting cells. Proc Natl Acad Sci U S A 118(30):e2023739118.

Thiel M, Wolfs MJ, Bauer S, *et al*., 2009. Efficiency of t-cell costimulation by cd80 and cd86 cross-linking correlates with calcium entry. Immunology 129(1): 28-40.

Thomas IJ, Petrich de Marquesini LG, Ravanan R, *et al*., 2007. Cd86 has sustained costimulatory effects on cd8 t cells. J Immunol 179(9): 5936-5946.

Vincenti F, 2008. Costimulation blockade in autoimmunity and transplantation. J Allergy Clin Immunol 121(2): 299-306; quiz 307-298.

Winter L, Ries J, Vogl C, *et al*., 2024. Comparative analysis of inhibitory and activating immune checkpoints pd-1, pd-l1, cd28, and cd86 in non-melanoma skin cancer. Cells 13(18):1569.

Yamada A, Salama AD and Sayegh MH, 2002. The role of novel t cell costimulatory pathways in autoimmunity and transplantation. J Am Soc Nephrol 13(2): 559-575.

Zhang Q, Ma R, Chen H, *et al*., 2023. Cd86 is associated with immune infiltration and immunotherapy signatures in aml and promotes its progression. J Oncol 2023: 9988405.

Zhang Q, Ma R, Chen H, *et al*., 2023. Cd86 is associated with immune infiltration and immunotherapy signatures in aml and promotes its progression. Journal of Oncology 2023: 1-19.

Zhao Y, Caron C, Chan YY, *et al*., 2023. Cis-b7:Cd28 interactions at invaginated synaptic membranes provide cd28 co-stimulation and promote cd8(+) t cell function and anti-tumor immunity. Immunity 56(6): 1187-1203 e1112.